Tree Counting by Bridging 3D Point Clouds with Imagery

Lei Li, Tianfang Zhang, Zhongyu Jiang, Cheng-Yen Yang, Jenq-Neng Hwang, Stefan Oehmcke,
Dimitri Pierre Johannes Gominski, Fabian Gieseke, Christian Igel
lilei@di.ku.dk

Abstract

Accurate and consistent methods for counting trees based on remote sensing data are needed to support sustainable forest management, assess climate change mitigation strategies, and build trust in tree carbon credits. Two-dimensional remote sensing imagery primarily shows overstory canopy, and it does not facilitate easy differentiation of individual trees in areas with a dense canopy and does not allow for easy separation of trees when the canopy is dense. We leverage the fusion of three-dimensional LiDAR measurements and 2D imagery to facilitate the accurate counting of trees. We compare a deep learning approach to counting trees in forests using 3D airborne LiDAR data and 2D imagery. The approach is compared with state-of-the-art algorithms, like operating on 3D point cloud and 2D imagery. We empirically evaluate the different methods on the NeonTreeCount data set, which we use to define a tree-counting benchmark. The experiments show that FuseCountNet yields more accurate tree counts.

1. Introduction

The accurate and efficient quantification of trees is critical in addressing climate change and advancing remote sensing technologies. By estimating tree biomass [6, 22, 26] or tree counts [1, 3, 15, 21], we can contribute to the mitigation of climate change and environment, while their spatial distribution data is fundamental to remote sensing applications. Understanding environmental dynamics through tree enumeration within expansive outdoor settings, utilizing remote sensing imagery [16], presents a valuable technique. Current tools for counting trees using 3D point cloud data in forests face limitations due to the scarcity of publicly accessible benchmark datasets specifically designed for tree counting from 3D LiDAR point clouds. Recently, two datasets have been proposed and helped develop new algorithms estimating tree numbers. YosemiteTree [3] encompasses a 10 square kilometer area, annotated with the coordinates of nearly 100 000 trees. In contrast, NeonTreeEvaluation [32] includes data collected from 22 different sites across the United States, employing multiple types of sensors.

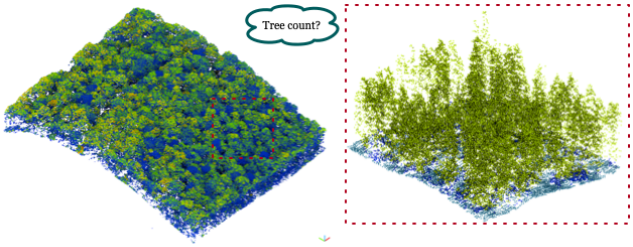

Figure 1. The task of quantifying objects directly from 3D point cloud data without any tree position information, such as tree count estimation in forest regions captured through remote sensing images. Figure (a) exhibits a 3D rendering of the point cloud data within a wooded area, whereas Figure (b) presents a frontal view of one part restricted to a 40m x 40m zone.

Tree counting methods based on images commonly apply detection models prior to the counting [28] or count the number of individual semantic segmentation masks [15, 21]. The detection models require to identify individual trees within an image, which can be challenging due to factors such as image quality and resolution, tree size, species diversity, and differences in lighting conditions [16]. In semantic segmentation approaches, distinguishing individual trees from the background is crucial yet challenging. This difficulty arises due to variations in tree crown shapes and sizes, the presence of shadows, and varying tree densities in images. Additionally, as noted in [15] and [32], the reliance on labor-intensive manual annotations, which are prone to ambiguity, can adversely affect the accuracy of tree counting.

Image-based methods, like [2] while simple and cost-effective, face difficulties in densely packed or partially occluded environments and struggle with challenges like variable tree sizes, canopy shapes, and overlapping crowns, highlighting the necessity for alternative techniques to enhance tree counting accuracy and efficiency. They primarily operate on 2D images and cannot fully capture the 3D structure of forests. In contrast, point cloud data, with its

rich attributes, notably height information, addresses the aforementioned image-based problem, making it invaluable for these kind of tasks. Methods for point cloud data offer the opportunity to derive more detailed and accurate insights from complex environmental data, further contributing to the academic and practical discourse. With the advancement of LiDAR technology, our work leverages the recent advancements in LiDAR technology to utilize 3D point clouds for tree counting tasks, a novel approach in this domain, providing a rich and previously unexplored source of information.

In this work, our objective is to harness the rich, inherently 3D information from LiDAR point clouds for a direct and efficient tree counting method, bypassing conventional intermediate tasks like detection or semantic segmentation. This approach is motivated by the need for a deeper understanding of forest ecosystems and the limitations of traditional image-based techniques, such as occlusions and shadows, as well as the reliance on manual annotations. By employing an innovative end-to-end method that utilizes point cloud data and label counts, we aim to enhance the accuracy of tree counting, thereby enabling more precise forest assessments and supporting informed environmental decision-making. This advancement in utilizing 3D point cloud data, detailed in Figure 1 and further corroborated by Magnussen et al. [20], not only represents a significant step forward in remote sensing applications but also contributes to combating climate change by providing a more accurate account of forest structures.

A pivotal consideration in our approach is the inherent uncertainty in aligning the bounding box in the image with the corresponding tree in the point cloud data. This ambiguity discourages the use of bounding boxes for tree detection as shown in Figure 2. Instead, we propose to eschew the intermediate step of bounding box detection and advocate for directly estimating the quantity of trees from the raw point cloud data. We utilize the whole tree bounding box number from the image to act as the count label of the 3D point cloud. Consequently, we propose a new task that focuses on counting objects, specifically trees, using raw 3D point cloud data as shown in Figure 1, termed NeonTreeCount. This simple approach aims to overcome the limitations of image-based counting methods without detection processing, such as issues related to occlusion, lighting variations, and the need for laborious manual annotations. By developing robust algorithms that can process and interpret 3D point cloud data, we aim to enhance the precision and scalability of tree counting. This new task not only represents an advancement in the domain of tree counting but also holds potential for far-reaching implications in areas such as climate change mitigation, forestry management, remote sensing, and environmental conservation.

Our work makes significant and varied contributions to the field, which are outlined below:

1. We conceptualize and propose a novel task for the enumeration of trees from LiDAR 3D point cloud data with a new 3D point cloud regression task.
2. We develop a novel and simple counting tree pipeline, called 3DTreeCountNet, which can enumerate trees in forest point cloud data, thus addressing and mitigating the challenges inherent in estimating tree populations in densely wooded areas without relying on any tree position supervision, making it highly practical and versatile for real-world applications.
3. Furthermore, we adapted a dataset, NeonTreeCount, within the realm of regression for 3D point cloud data. This dataset not only serves as a practical resource for our research but also establishes an experimental benchmark for the application of deep learning methodologies in this specific field.

These contributions collectively enhance the discourse on object counting methodologies, particularly in the context of 3D point cloud data, and pave the way for more refined and accurate studies in the future.

2. Related Works

Image-based Object Counting. Object Counting estimates the number of objects in dense scenarios for tasks such as crowd counting, vehicle counting, plant counting, cell counting, and livestock counting from images. Previous image-based counting can be categorized into three main techniques: (1) counting-by-detection [19, 29, 31], (2) counting-by-regression [17], and (3) density-map-based approaches [7, 18, 24, 33]. Counting-by-detection refers to the method to take advantage of the detector and then simply count the number of detected bounding boxes; the high localization abilities of the detector enable us to obtain the spatial information of our targets but will often fail when dealing with crowd scenes.

Counting-by-regression methods in object counting are categorized into patch-level and pixel-level regression. The latter, particularly effective in crowd counting, uses advanced density maps like distance-label [33], Focal Inverse Distance Transform (FIDT) [18], and Independent Instance Map (IIM) [7] to improve accuracy and avoid overlaps, albeit with increased complexity and post-processing needs.

3D Point Cloud Regression Tasks. The application of segmentation, detection, classification, and regression tasks using a 3D point cloud has emerged as a promising area in recent years. Point-based[25, 25], kernel point based [30] and voxel-based [4, 5] have been proposed for 3D point cloud representation learning. Despite the growing body of research in point cloud processing, direct regression tasks on point cloud data, such as estimating the biomass/tree vol-

ume [10, 22, 23, 26], remain relatively unexplored. These tasks, which involve leveraging deep learning techniques to infer quantitative measures directly from point cloud data, represent a critical and emerging subfield within the broader domain of point cloud analyses. The scarcity of work in this area signifies the innovative nature of these tasks and their potential to significantly contribute to our understanding and utilization of point cloud data.

Tree Counting. Counting trees is crucial for bio-diversity monitoring, carbon sequestration assessment, and effective forest management, underscoring its environmental and ecological significance. Within the domain of remote sensing, the task of counting trees has been approached via several methodologies. These encompass traditional image-based techniques, where pixel-level segmentation [1, 14, 21] and object detection [3, 32] methods are employed to identify and count individual trees. Image segmentation [11–13, 13] or detection, a prevalent approach, divides an image into regions or segments, can use for corresponding to an individual tree, then sum up to the tree count. Martin *et al*. [1] utilize submetre-resolution satellite imagery and image segmentation, over 1.8 billion isolated dryland trees, to map across 1.3 million km² in West Africa, challenging prevailing desertification narratives with a U-Net [27] structure. Ben *et al*. [32] outlines a semi-supervised tree detection approach to effectively identify tree crowns in RGB imageries from remote sensing. Li *et al*. [15] rely on the tree position to count the tree based on kernel deep sampling.

3. Methods

3.1. Problem Formulation

Comparing the research field of deep learning for point cloud data to deep convolutional neural networks (CNNs) for conventional 2D images and 3D voxel images, it becomes evident that it has yet to achieve the same level of maturity, especially regression tasks for 3D point cloud. Numerous strategies exist to modify neural networks for point cloud processing, each dealing differently with the essential question of how to extend the notion of spatial convolutions to sparse point clouds. Majority of deep learning systems for point clouds are developed with a focus on segmentation and detection. The new task of computing objects with 3D point cloud regression will enrich some scenarios under 3D understanding.

Consider a three-dimensional point cloud dataset $\mathcal{P} = p_i i = 1^N$, where each point $p_i = (x_i, y_i, z_i)$ is confined within a region defined by width w and height h. For the points in $\mathcal{P}$, we have a corresponding set of labels $C = c_i i = 1^N$. Beyond coordinates, points in $\mathcal{P}$ may have additional attributes like color or intensity. We aim to use a network function F, parameterized by θ, to process $\mathcal{P}$. The output of this network, denoted as $\hat{C} = F(\mathcal{P}; \theta)$, provides label estimations. The goal is to optimize θ so that $\hat{C}$ approximates the true labels C, achievable by minimizing a loss function $L(C, \hat{C})$.

Figure 1 furnishes a detailed illustration of the dataset, emphasizing the complex spatial architecture encapsulated within the point cloud, and invokes the challenge of deriving tree counts directly from this point cloud data. Successively, Figure 2b delivers a comprehensive perspective of the 3D point cloud, which, upon being superimposed onto the matching point cloud data, produces Figure 2a with an encapsulation of point cloud annotations housed in bounding boxes. It is pivotal to recognize the possibility of misalignment between the image and its corresponding point cloud, a deviation that becomes more noticeable when viewed from a bird's eye perspective, and using bounding boxes for tree representation is suboptimal, especially for trees with a predominantly round shape, as this method may not accurately capture their true dimensions and form. Fundamentally, this research aims to infer tree counts directly from point cloud data, thereby detaching the task of synchronizing specific tree bounding boxes within the point cloud. Our pipeline in Figure 5 solely processes raw data: the individual point coordinates (x, y, z) and the tree count.

3.2. Data

We adapt the NeonTreeEvaluation Benchmark dataset [32] to serve a new task: 3D point cloud counting, termed as NeonTreeCount Benchmark dataset. First, we split the NeonTreeEvalution dataset with labelled information as train split with 600 samples and test split with 150 samples. Then, because the NeonTreeEvaluation dataset contains detection bounding boxes, we sum the number of tree detection bounding boxes as the count label of the trees. In this way, we have the corresponding 3D LiDAR data with the count label, which is termed as NeonTreeCount dataset. Further details and specific samples are referred in the supplementary materials.

Figure 2 and Figure 3 also highlight the varying density of the point cloud across different regions. This variability stems from the diverse heights of the trees, making the tree-related characteristics prominently discernible in areas with tree presence. Accordingly, we propose to leverage such data and design a novel network. The primary objective of this network would be to extract distinct tree features and count tree clusters, thus facilitating a more direct and accurate estimation of tree numbers. As visualized in the subplots of Figure 3, an equidistant frontal plot, with a specified length and width of 40m (the height is naturally determined by the trees themselves) is displayed. The corresponding numerical value represents the count of trees within each subplot.

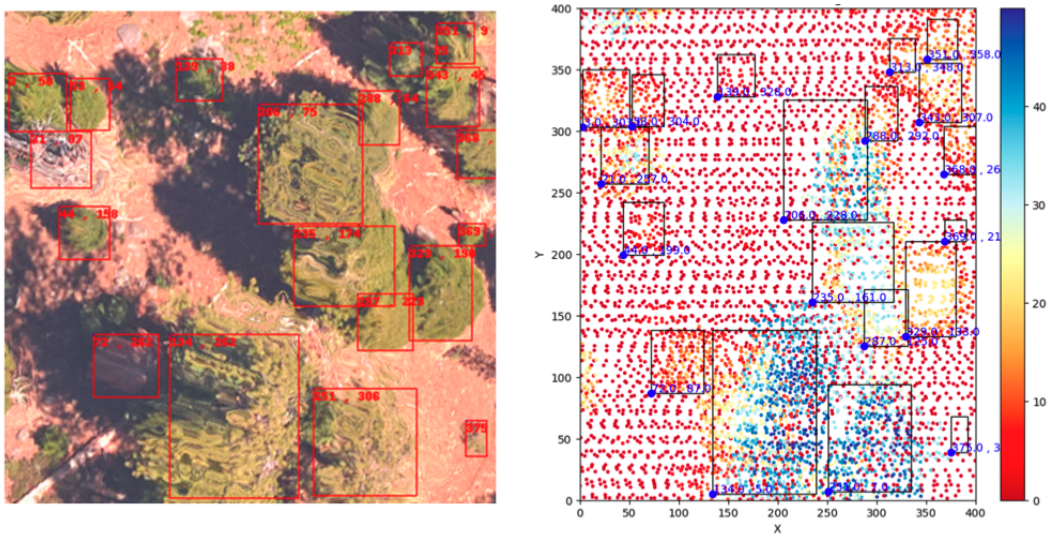

(a) Bird's-Eye-View image with bounding box

(b) Bird's-Eye-View 3D point cloud with Projection bounding box

Figure 2. (a) Illustrates the bird's-eye-view image, accompanied by bounding boxes; (b) Displays the bird's-eye-view of the point cloud, incorporating projected image bounding boxes. The color spectrum represents the variation in the point cloud's height.

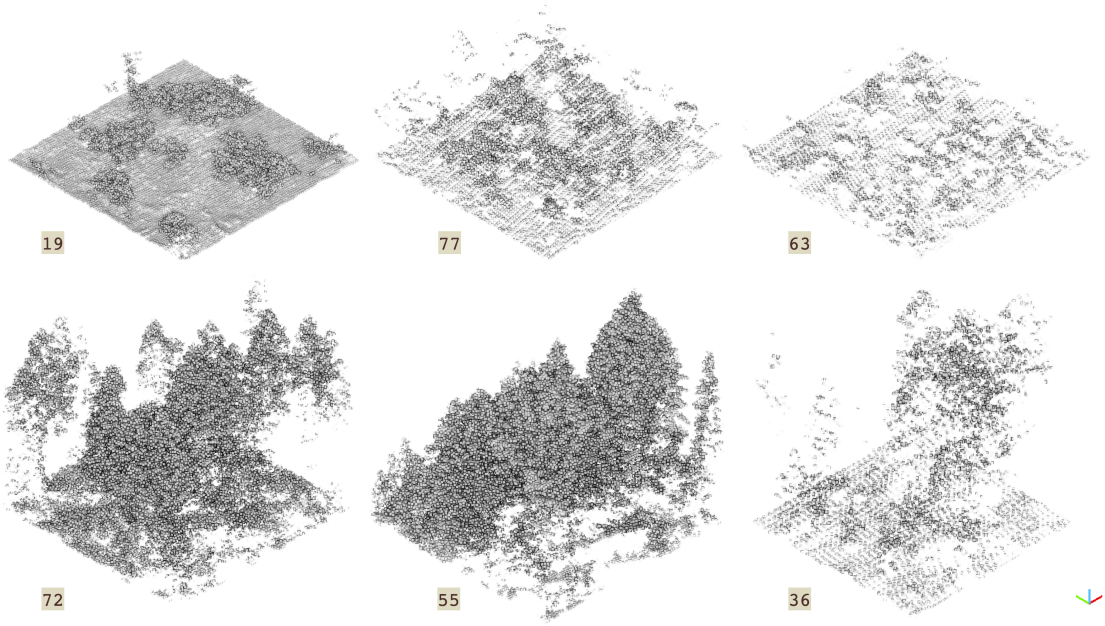

Figure 3. This figure presents various subplots, each containing a different number of trees. The points depicted correspond to trees and the ground with isometric front perspective respectively.

3.3. Overview

As mentioned in Section 3.1, the illustration represents our 3DTreeCountNet pipeline, which leverages airborne LiDAR-acquired 3D point cloud data to enumerate trees using a deep learning network. This framework encapsulates our novel approach to tree count estimation utilizing 3D geospatial point cloud data.

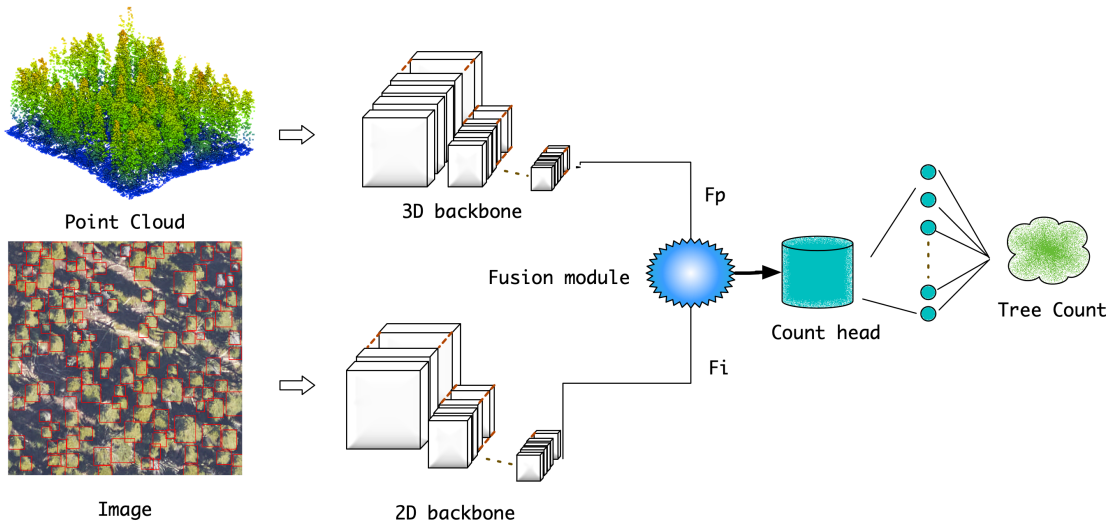

Figure 4

$$\mathcal{P} = \{p_i\}_{i=1}^{N}, p_i = (x_i, y_i, z_i) \in \mathbb{R}^3, C = \{c_i\}_{i=1}^{N} \quad (1)$$

$$\hat{C} = F(\mathcal{P}; \theta) \quad (2)$$

$$\theta^* = \arg\min_{\theta} L(C, \hat{C}) \quad (3)$$

$$\theta \leftarrow \theta - \eta \nabla_\theta L(C, \hat{C}) \quad (4)$$

The methodology employed involves feeding four-dimensional data - comprising of the (x, y, z) coordinates for each point and the overall count of trees within the area - directly into our computational pipeline. Subsequently, the network learns to perform regression on the tree count. This approach facilitates an efficient and straightforward estimation of the number of trees from the point cloud data. It signifies the efficiency and simplicity of our approach to tree count estimation directly from point cloud data.

3.4. Network

In this section, we delve into the specific network architecture employed in our tree counting task within the context of the 3D point cloud. As an example, the foundational Minkowski network [5] executes grid voxel sampling to obtain a voxel representation corresponding to a 40m*40m point cloud. In contrast, the PointNet methodology procures corresponding values through point-by-point random sampling. Our proposed solution, 3DTreeCountNet, adopts a voxel-based approach. We set a grid for voxel sampling, which aligns with the goal of efficiently processing the 3D point cloud data for tree counting.

After implementing grid sampling and obtaining the voxel, we deploy a Sparse3D convolutional network to extract information pertinent to the corresponding voxel. The Sparse3D convolutional network, characterized by kernels of sizes 7 and 3, is integrated into the Max Pooling layer to generate a voxel feature representation that encapsulates salient information. The design of our 3D block culminates in passing the output through a fully connected layer and subsequently a linear regression model, to compute our desired value.

In the development of our 3D block, it's important to emphasize that we adopt methodologies rooted in ResNet and Squeeze-and-Excitation Networks (SENet) frameworks [9]. As an illustration, the SENet-based model incorporates a skip connection layer subsequent to three layers of SparseConv, which effectively amalgamates multi-scale information. The salience of this amalgamation is best seen post-Max Pooling, where it adeptly extracts feature information. Furthermore, within our pipeline, we incorporate a fusion of features and 3D blocks post-sampling, which significantly enhances the efficacy of representation learning within the entirety of the point cloud.

3.4.1 Fusion module

For fusion module design, as the figure **??** shows, The proposed model integrates the point cloud feature map with image feature information through a fusion process tailored for counting applications. Initially, the model harnesses a modified 3D point cloud encoder network, such as PointNet or SENet, to extract spatially encoded point features from the input point cloud, alongside an aggregated global feature. To adapt this network to the specifics of 3D regression tasks, we eliminate the batch normalization layers from the original PointNet architecture. The fusion of these two modalities is facilitated by the point cloud-to-image position ma-

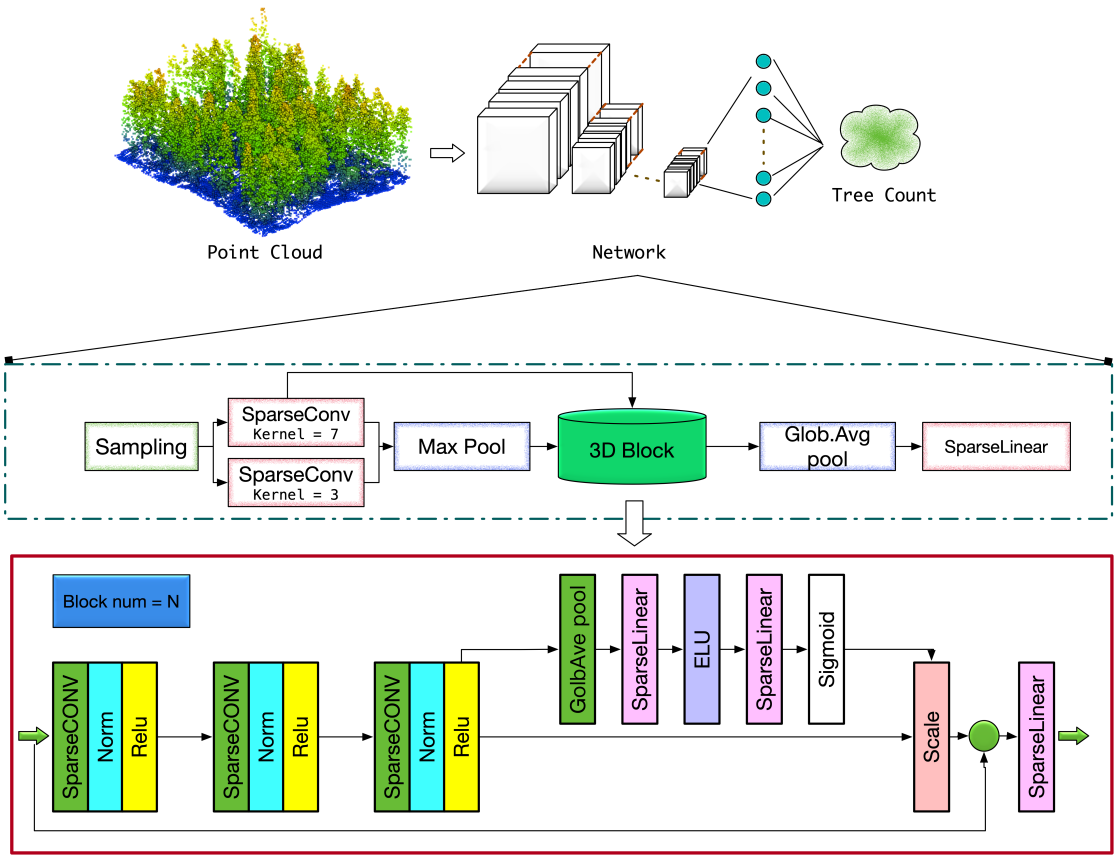

Figure 5. Our 3DTreeCountNet pipeline. We use 3D point cloud from airborne LiDAR to count the trees using a deep learning network. A 3D rendering is employed to visualize the points, with green signifying vegetation points and blue designating the ground. Our network contains sampling, multi-scale sparse convolutions and 3D Blocks. We design several 3D Blocks, including point-based, kernel-point based, and voxel-based. The red rectangle shows the block of the SENet with block number one.

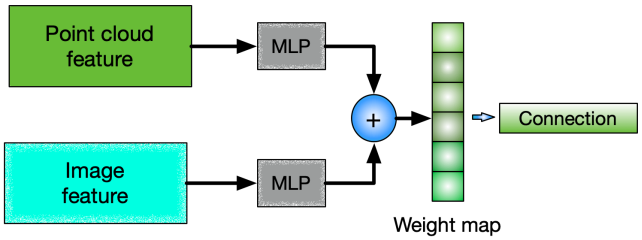

Figure 6. Fuse.

trix M. This matrix projects the sampled point cloud onto the corresponding locations within the image feature map or RGB image, following the projection equation:

$$p' = M \times p \tag{5}$$

where M denotes the projection matrix, p is the point cloud after cropping or fusion sampling, and p' signifies the projected point position on the feature map.

Post projection, the image features at the corresponding points are extracted to represent the point cloud semantically. For each point, an image feature vector is generated, using the image feature map F and the image sampling location p' as inputs. To obtain the image features at continuous coordinates, bilinear interpolation is applied as per the following equation:

$$F_I(p) = B(f(N(p'))) \tag{6}$$

where $F_I(p)$ represents the interpolated image feature, N denotes the nearest neighbor function providing the closest point p' on the feature map, f extracts the feature vector at p', and B signifies the bilinear interpolation function. Subsequently, a fusion layer with self-attention weights is introduced to adaptively estimate the importance of image feature contributions to the LIDAR features. An MLP first maps the point cloud features F_P and the RGB image features F_I to a uniform dimensionality, combining them to form an implicit feature representation. The weight map W is then obtained through another MLP and normalized via an activation function:

$$w = \sigma(W \times \tanh(U \times F_P + V \times F_I)) \quad (7)$$

where W, U, and V are the learned weight coefficients, σ represents the sigmoid activation function, and F_P, F_I are the features from the point cloud and RGB images, respectively. These weights, confined within the range $[0, 1]$, balance the contribution of LIDAR and image features in the final fused representation.

4. Experiments

4.1. Metric

We conduct a rigorous comparative analysis of methodologies aimed at predicting counting, which consequently enables the estimation of the count of the trees. Our analytical techniques capitalized on different statistical metrics: The Coefficient of Determination (R^2), defined as:

$$R^2 = 1 - \frac{\sum_{i=1}^{N} \left(C_i - \hat{C}i\right)^2}{\sum i = 1^N \left(C_i - \frac{\sum_{j=1}^{N} C_j}{N}\right)^2} \quad . \quad (8)$$

The Root Mean Square Error (RMSE), is formulated as:

$$\text{RMSE} = \sqrt{\frac{1}{N}\sum_{i=1}^{N}\left(C_i - \hat{C}_i\right)^2} \quad . \quad (9)$$

Lastly, we also evaluated the mean error:

$$\text{Mean Error} = \frac{1}{N}\left|\sum_{i=1}^{N} C_i - \hat{C}_i\right|, \quad (10)$$

which allows us to further highlight discrepancies in aggregated predictions.

4.2. Quantitative analysis

We base on stat-of-art method Tree Mapping [8] to have a thorough comparison with our 3DTreeCountNet shown in Table 1 and Table 2

We also fuse the representation of point cloud and image for the counting task.

Our investigation has focused on the qualitative and quantitative aspects of using point cloud data for the direct regression of learning tree counts. The results shown in Table 2 clearly indicate the high effectiveness of our approach. The top portion of the table displays regression outcomes of the ResNet and SENet networks when applied to associated images. The relative ineffectiveness of this approach could potentially stem from numerous occlusions present in the aerial view of the forest and complications related to data resolution.

The lower part of the table, conversely, demonstrates the regression results obtained directly from the point cloud data. For this purpose, we employ the point-based PointNet and KPConv, setting the kernel point number to 15 in the latter. A key insight from our analysis is that tree count predictions can be significantly enhanced by harnessing multi-scale learning of Voxel-based sparse 3D. This represents the potential of three-dimensional data and learning techniques in improving prediction accuracy in ecological scenarios.

We have further validated our methodology by plotting the prediction and corresponding ground truth with 40 samples for visualizing better. The accompanying Figure 8 illustrates this, with the x-axis representing the model's predicted values and the y-axis representing the actual label values. Our proposed framework, 3DTreeNet, demonstrates impressive efficacy in predicting an accurate count of trees, irrespective of variations in forest density. This includes regions with sparser tree populations. To conclude, our findings illuminate the considerable potential of leveraging 3D point cloud data and sophisticated machine learning methods for ecological forecasting. This analytical visualization serves to establish a correlation between predictive and actual counts, providing a comprehensive evaluation of the predictive model's performance. Such techniques can undoubtedly propel future advancements in forestry analytics and decision-making.

4.3. Qualitative Analysis

The study results are visually demonstrated through an organized representation of performance output on the test data as shown in Figure 7. The far-right column showcases the original images corresponding to the data. Although these images serve to enhance the viewer's understanding and perception, it should be noted that they are not actively utilized in the research process outlined in this paper. The subsequent three columns represent various perspectives: front view, bird's eye view, and side view, thereby providing a multi-faceted visualization of the data. These three views are respectively illustrated in three distinct tree density scenarios, represented by (a), (b), and (c). Upon reviewing these outcomes, it becomes evident that our model demonstrates a compelling capacity to effectively estimate the number of trees encapsulated within the point cloud data, thus validating the efficacy of our proposed task in various tree density conditions.

4.4. Ablation Study

As shown in Table 3, we investigate the efficiency of varying block numbers. We designed several 3D blocks integrated with SENet for this study. The results indicate that the optimal performance is achieved when the number of blocks is set to four.

This finding suggests a potential relationship between the number of blocks and the network's effectiveness, where a balance must be struck to avoid overfitting. The potential

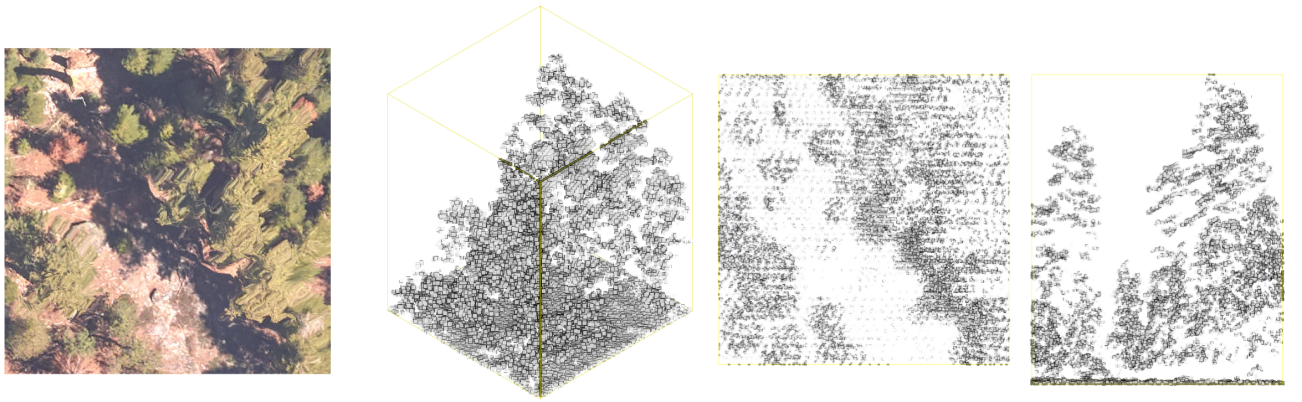

(a) Tree count Estimation with 36; Groundtruth count with 39

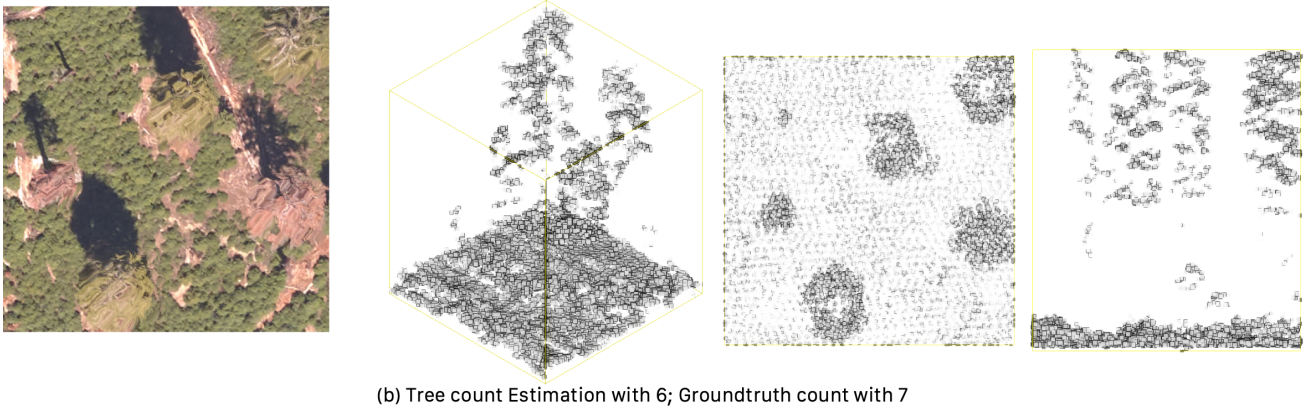

(b) Tree count Estimation with 6; Groundtruth count with 7

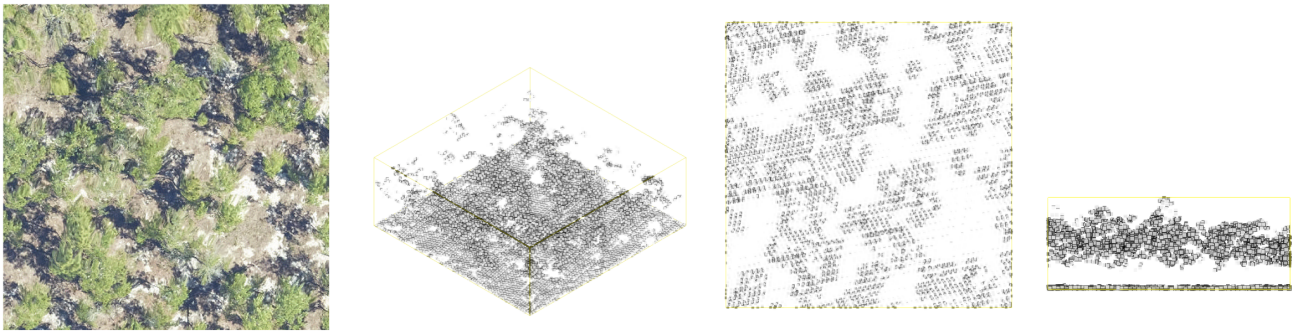

(c) Tree count Estimation with 69; Groundtruth count with 63

Figure 7. The analysis of the performance output on the test data is succinctly represented through a series of depictions. The initial column on the right showcases the original images corresponding to the point cloud data, providing a visual context, albeit these images are not used as inouts to our model. The ensuing three columns provide three distinct perspectives of the data: a frontal view, a bird's eye view, and a lateral side view, respectively

for overfitting could be elevated with larger networks, particularly considering the dimensions of our dataset. Hence, choosing an appropriate number of blocks is critical to ensure the effectiveness of the model while mitigating the risk of overfitting.

5. Discussion

In this study, we highlight a new task centered on employing 3D point cloud data for estimating tree counts. It is crucial to mention that our dataset comprises bounding box labels and point cloud classification, which facilitates additional explorations like predicting localization and extract-

Table 1. Experimental Results Based on Tree Mapping [8] with 2D image

Experiment	**MAE**	**R2**	**RMSE**	**Threshold**	**NMS Kernel Size**
Training Parameters	14.4634	0.9614	33.9336	0.6	9
Best MAE	12.5366	0.9669	31.3905	0.4	27
Best RMSE	13.4146	0.9733	28.2169	0.5	29
Best R2	13.4146	0.9733	28.2169	0.5	29

Data	Method	MAE ↓	RMSE ↓	R^2 ↑
Image-based	Resnet18	15.596	26.568	0.6547
	Resnet50	14.874	24.368	0.6854
	SENet50	15.425	26.576	0.6658
	TreeMaping [8]	12.5366	0.9669	31.3905
LiDAR-based	PointNet	20.322	26.567	0.5642
	KPConv	12.378	20.617	0.6767
	SENet18	7.636	13.992	0.8511
	SENet50	7.553	11.617	0.8142
	3DTreeCountNet	7.193	10.401	0.9117
Lidar & Image	FuseCountNet	**7.012**	**9.787**	**0.9202**

Table 2. Counting errors of different regression approaches on the NeonTreeCount Dataset. The bold numbers represent the best performance in each column with regression methods.

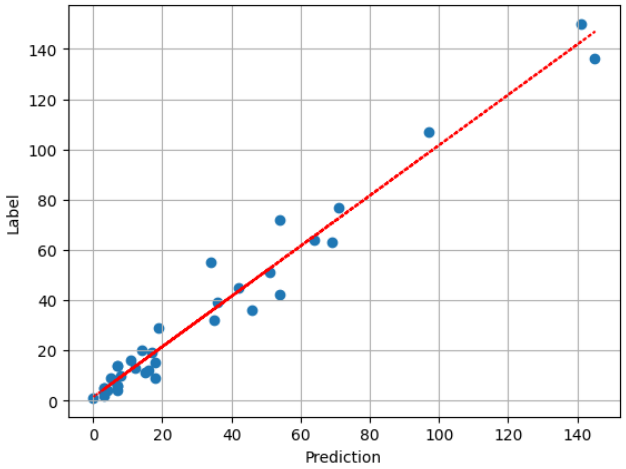

Figure 8. The graph presents the numerical results derived from parts of the test set, whereby the manually counted labels correspond to the predicted counts. The horizontal axis represents the predicted values, while the vertical axis depicts the values obtained from the labels. .

ing image textures. Nevertheless, it must be recognized that current methods predominantly use 2D images, usually of greater sizes compared to LiDAR data. Consequently, our comparison indicates the feasibility of directly estimating tree counts using 3D raw point cloud data, despite not offering an entirely exhaustive comparison.

Our current approach is to investigate the utility of fusing point cloud and image data for counting tasks. There exists, however, a breadth of possibilities for exploring the alignment between point cloud and image data. This could include, for instance, the implementation of attention mechanisms to enhance the interplay between the two data modalities.

Block Num	MAE ↓	RMSE ↓	R^2 ↑
1	9.841	17.586	0.7647
2	9.454	16.593	0.7906
3	7.636	13.992	0.8511
4	**7.193**	**10.401**	**0.9117**
5	8.157	12.156	0.8377

Table 3. Counting errors of different approaches on the NeonTreeEvaluation Dataset. The bold numbers denote the best performance in each column.

Given the constraints of the data size, our current network demonstrates efficient performance for this dataset. In future work, if similar point cloud data become available, we are well-positioned to execute further experiments and tests. From a theoretical standpoint, the availability of larger volumes of data could enhance the efficacy of the model. This potential avenue of exploration could not only validate our current results, but also provide the opportunity to fine-tune our model for broader and more diverse applications.

6. Conclusion

We introduce a novel and potentially transformative methodology for object enumeration in forest landscapes using LiDAR 3D point cloud data. Our work primarily emphasizes the development and implementation of the 3DTreeCountNet framework, a simple yet effective tool designed to count trees directly from point cloud data. The results demonstrate a significant advancement in object counting tasks, thus widening the horizons of 3D point cloud representation learning. Our innovative task, which involves tree enumeration from LiDAR 3D point cloud data, adds a new dimension to quantitative methodologies in this field. The 3DTreeCountNet pipeline, meticulously designed to address the challenges inherent in estimating tree populations in densely wooded areas, represents a major stride in forest analytics. Moreover, the introduction of the NeonTreeCount dataset creates a benchmark for 3D point cloud data, propelling the application of deep learning method-

ologies in this area. These findings represent a significant milestone in the convergence of deep learning and environmental research, and we are optimistic about their impact on future studies in forestry analytics and ecological decision-making.

References

[1] Martin Brandt, Compton J Tucker, Ankit Kariryaa, Kjeld Rasmussen, Christin Abel, Jennifer Small, Jerome Chave, Laura Vang Rasmussen, Pierre Hiernaux, Abdoul Aziz Diouf, et al. An unexpectedly large count of trees in the west african sahara and sahel. *Nature*, 587(7832):78–82, 2020. 1, 3

[2] Likun Cai, Zhi Zhang, Yi Zhu, Li Zhang, Mu Li, and Xiangyang Xue. Bigdetection: A large-scale benchmark for improved object detector pre-training. In *Proceedings of the IEEE/CVF Conference on Computer Vision and Pattern Recognition*, pages 4777–4787, 2022. 1

[3] Guang Chen and Yi Shang. Transformer for tree counting in aerial images. *Remote Sensing*, 14(3):476, 2022. 1, 3

[4] Yukang Chen, Jianhui Liu, Xiangyu Zhang, Xiaojuan Qi, and Jiaya Jia. Voxelnext: Fully sparse voxelnet for 3d object detection and tracking. In *Proceedings of the IEEE/CVF Conference on Computer Vision and Pattern Recognition*, pages 21674–21683, 2023. 2

[5] Christopher Choy, JunYoung Gwak, and Silvio Savarese. 4d spatio-temporal convnets: Minkowski convolutional neural networks. In *Proceedings of the IEEE/CVF conference on computer vision and pattern recognition*, pages 3075–3084, 2019. 2, 5

[6] Aida Cuni-Sanchez, Martin JP Sullivan, Philip J Platts, Simon L Lewis, Rob Marchant, Gérard Imani, Wannes Hubau, Iveren Abiem, Hari Adhikari, Tomas Albrecht, et al. High aboveground carbon stock of african tropical montane forests. *Nature*, 596(7873):536–542, 2021. 1

[7] Junyu Gao, Tao Han, Yuan Yuan, and Qi Wang. Learning independent instance maps for crowd localization. *CoRR*, abs/2012.04164, 2020. 2

[8] Dimitri Gominski, Ankit Kariryaa, Martin Brandt, Christian Igel, Sizhuo Li, Maurice Mugabowindekwe, and Rasmus Fensholt. Benchmarking individual tree mapping with sub-meter imagery, 2023. 7, 9

[9] Jie Hu, Li Shen, and Gang Sun. Squeeze-and-excitation networks. In *Proceedings of the IEEE conference on computer vision and pattern recognition*, pages 7132–7141, 2018. 5

[10] Lei Li. Hierarchical edge aware learning for 3d point cloud. In *Computer Graphics International Conference*, pages 81–92. Springer, 2023. 3

[11] Lei Li. Segment any building. In *Computer Graphics International Conference*, pages 155–166. Springer, 2023. 3

[12] Lei Li. Cpseg: Finer-grained image semantic segmentation via chain-of-thought language prompting. In *Proceedings of the IEEE/CVF Winter Conference on Applications of Computer Vision*, pages 513–522, 2024.

[13] Lei Li, Tianfang Zhang, Zhongfeng Kang, and Xikun Jiang. Mask-fpan: Semi-supervised face parsing in the wild with de-occlusion and uv gan. *Computers & Graphics*, 116:185–193, 2023. 3

[14] Lei Li, Tianfang Zhang, Stefan Oehmcke, Fabian Gieseke, and Christian Igel. Buildseg buildseg: A general framework for the segmentation of buildings. *Nordic Machine Intelligence*, 2(3), 2022. 3

[15] Sizhuo Li, Martin Brandt, Rasmus Fensholt, Ankit Kariryaa, Christian Igel, Fabian Gieseke, Thomas Nord-Larsen, Stefan Oehmcke, Ask Holm Carlsen, Samuli Junttila, et al. Deep learning enables image-based tree counting, crown segmentation, and height prediction at national scale. *PNAS nexus*, 2(4), 2023. 1, 3

[16] Weijia Li, Runmin Dong, Haohuan Fu, and Le Yu. Large-scale oil palm tree detection from high-resolution satellite images using two-stage convolutional neural networks. *Remote Sensing*, 11(1):11, 2018. 1

[17] Dingkang Liang, Wei Xu, and Xiang Bai. An end-to-end transformer model for crowd localization. *European Conference on Computer Vision*, 2022. 2

[18] Dingkang Liang, Wei Xu, Yingying Zhu, and Yu Zhou. Reciprocal distance transform maps for crowd counting and people localization in dense crowd. *CoRR*, abs/2102.07925, 2021. 2

[19] Yuting Liu, Miaojing Shi, Qijun Zhao, and Xiaofang Wang. Point in, box out: Beyond counting persons in crowds. In *Proceedings of the IEEE/CVF Conference on Computer Vision and Pattern Recognition (CVPR)*, June 2019. 2

[20] Steen Magnussen, Thomas Nord-Larsen, and Torben Riis-Nielsen. Lidar supported estimators of wood volume and aboveground biomass from the Danish national forest inventory (2012–2016). 211:146–153, 2018. 2

[21] Maurice Mugabowindekwe, Martin Brandt, Jérôme Chave, Florian Reiner, David L Skole, Ankit Kariryaa, Christian Igel, Pierre Hiernaux, Philippe Ciais, Ole Mertz, et al. Nation-wide mapping of tree-level aboveground carbon stocks in rwanda. *Nature Climate Change*, 13(1):91–97, 2023. 1, 3

[22] Stefan Oehmcke, Lei Li, Jaime C Revenga, Thomas Nord-Larsen, Katerina Trepekli, Fabian Gieseke, and Christian Igel. Deep learning based 3d point cloud regression for estimating forest biomass. In *Proceedings of the 30th International Conference on Advances in Geographic Information Systems*, pages 1–4, 2022. 1, 3

[23] Stefan Oehmcke, Lei Li, Katerina Trepekli, Jaime C Revenga, Thomas Nord-Larsen, Fabian Gieseke, and Christian Igel. Deep point cloud regression for above-ground forest biomass estimation from airborne lidar. *Remote Sensing of Environment*, 302:113968, 2024. 3

[24] Daniel Onoro-Rubio and Roberto J López-Sastre. Towards perspective-free object counting with deep learning. In *Computer Vision–ECCV 2016: 14th European Conference, Amsterdam, The Netherlands, October 11–14, 2016, Proceedings, Part VII 14*, pages 615–629. Springer, 2016. 2

[25] Charles R Qi, Hao Su, Kaichun Mo, and Leonidas J Guibas. Pointnet: Deep learning on point sets for 3d classification and segmentation. In *Proceedings of the IEEE conference on computer vision and pattern recognition*, pages 652–660, 2017. 2

[26] Jaime C Revenga, Katerina Trepekli, Stefan Oehmcke, Rasmus Jensen, Lei Li, Christian Igel, Fabian Cristian Gieseke, and Thomas Friborg. Above-ground biomass prediction for

croplands at a sub-meter resolution using uav–lidar and machine learning methods. *Remote Sensing*, 14(16):3912, 2022. 1, 3

[27] Olaf Ronneberger, Philipp Fischer, and Thomas Brox. U-net: Convolutional networks for biomedical image segmentation. In *Medical Image Computing and Computer-Assisted Intervention–MICCAI 2015: 18th International Conference, Munich, Germany, October 5-9, 2015, Proceedings, Part III 18*, pages 234–241. Springer, 2015. 3

[28] Stefan Schmohl, Alejandra Narváez Vallejo, and Uwe Soergel. Individual tree detection in urban als point clouds with 3d convolutional networks. *Remote Sensing*, 14(6):1317, 2022. 1

[29] Qingyu Song, Changan Wang, Zhengkai Jiang, Yabiao Wang, Ying Tai, Chengjie Wang, Jilin Li, Feiyue Huang, and Yang Wu. Rethinking counting and localization in crowds: A purely point-based framework. 2021. 2

[30] Hugues Thomas, Charles R Qi, Jean-Emmanuel Deschaud, Beatriz Marcotegui, François Goulette, and Leonidas J Guibas. Kpconv: Flexible and deformable convolution for point clouds. In *Proceedings of the IEEE/CVF international conference on computer vision*, pages 6411–6420, 2019. 2

[31] Yi Wang, Junhui Hou, Xinyu Hou, and Lap-Pui Chau. A self-training approach for point-supervised object detection and counting in crowds. *IEEE Transactions on Image Processing*, 30:2876–2887, 2021. 2

[32] Ben G Weinstein, Sergio Marconi, Stephanie Bohlman, Alina Zare, and Ethan White. Individual tree-crown detection in rgb imagery using semi-supervised deep learning neural networks. *Remote Sensing*, 11(11):1309, 2019. 1, 3

[33] Chenfeng Xu, Dingkang Liang, Yongchao Xu, Song Bai, Wei Zhan, Xiang Bai, and Masayoshi Tomizuka. Autoscale: Learning to scale for crowd counting. *International Journal of Computer Vision*, 130:1–30, 02 2022. 2